JOURNAL OF MATERIALS SCIENCE 11 (1976) 224–230

Surface free energy of nickel and stainless steel at temperatures above the melting point

U. M. AHMAD, L. E. MURR
Department of Metallurgical and Materials Engineering, New Mexico Institute of Mining and Technology, Socorro, New Mexico, USA

The surface tension (liquid-state surface free energy) of pure nickel and type 304 stainless steel was measured in a narrow temperature range above the melting point by the sessile drop method. The temperature coefficients of surface free energy in the liquid state were found to be $-1.76\,\text{erg cm}^{-2}\,^{\circ}\text{C}^{-1}$ for nickel and $-2.48\,\text{erg cm}^{-2}\,^{\circ}\text{C}^{-1}$ for stainless steel. These values are shown to be a factor of 2 larger than those previously determined for the solid surface free energies of nickel and stainless steel, but have the same sign. The latent heats of fusion of nickel and 304 stainless steel were determined by comparison of variations of solid and liquid-state surface energies with temperature and found to be 292 and 284 erg cm^{-2} respectively. Measurement of the contact angle for a nickel sessile drop on thoria and a stainless steel sessile drop on alumina showed a decrease in the angle with an increase in temperature.

1. Introduction

Measurements of the surface tension (or surface free energy in the liquid state) of numerous metals and some alloys have been made over several decades utilizing sessile drop methods where a liquid metal or alloy drop resting on a solid (usually ceramic) assumes an equilibrium shape depending upon interfacial and gravitational forces acting on the drop [1]. The method most popularly employed in the case of drops larger than 1 cm consists of calculating the surface tension and contact angle from mean measurements of the drop geometrical parameters utilizing empirical relations and tables developed by Bashforth and Adams [2] and modified by Dorsey [3] (e.g. Humenik and Kingery [4] and Allen and Kingery [5]). For drops smaller than 1 cm, this method is inaccurate because of the lack of gravitational flattening of the drop [6] and the surface tension is evaluated from the simple relationship

$$\gamma_{LV} = Dd_m^2\rho g, \qquad (1)$$

where D is a geometrical factor which depends upon the ratio of the maximum drop diameter, d_m to the height of the drop summit from this diameter, H, as shown in Fig. 1; ρ and g are the drop density and gravitational constant respectively. Koshavnik *et al.* [7] have prepared an extensive table relating d with $d_m/2H$ and have discussed the applicability of Equation 1 to small sessile drops (<1 cm).

The geometrical-interfacial phenomena implicit in Fig. 1 have also been shown to be applicable in solid-state measurements of contact angle and

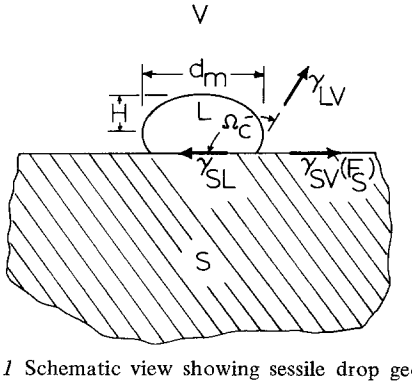

Figure 1 Schematic view showing sessile drop geometry and associated equilibrium interfacial energies. The contact angle is denoted Ω_c.

interfacial free energies [8, 9]. The applications of this method to calculations of adhesive energies have also been shown to be simple and straightforward [1].

Except for the earlier work of Allen and Kingery [5], little additional work has been done in attempting to evaluate the surface free energy of metals within a narrow temperature range extending above and below the melting point, and there do not appear to have been any attempts to evaluate the surface free energy of an alloy near the solid–liquid transition. Consequently, there is little information available from which a description of adhesive energy above and below the melting point (including the solid–liquid transition) can be made as a function of temperature.

A more fundamental understanding of the mechanism of adherence and the factors influencing metal distribution in ceramics as well as metal–ceramic interfaces can be obtained by investigating metal and alloy surface tensions and the associated wettability of metal–ceramic systems. Furthermore, the control of interfacial free energies and related interfacial phenomena can only be accomplished when sufficient information establishing the fundamentals involved is known. This information becomes increasingly valuable at temperatures near the melting point where in metal–ceramic systems local changes of state at an interface must lead in some cases to catastrophic consequences as a result of decohesion at the boundary or interfacial region.

The present experimental programme was undertaken in part in an effort to provide certain information as outlined above, and in part to answer more fundamental thermodynamic questions relating directly to the concept of surface free energy in the liquid and solid states. In particular since the temperature coefficient, $d\gamma/dT$, for a pure metal must always be negative in the absence of surface contamination, it was desired to measure the temperature coefficient for pure Ni since recent measurements of contaminated Ni had shown a positive value for $d\gamma_{LV}/dT$ above the melting point [10]. In addition, since the solid surface free energy of Ni has been established as a function of temperature [1], it was recognized that the solid–liquid surface energy transition could be investigated and the associated heat of fusion evaluated. It has been shown that the temperature coefficient of surface energy for solid 304 stainless steel is also negative as in pure metals [11], and the present experiments were also undertaken in an effort to determine the continuation of this trend in the liquid state.

More fundamentally, it was desired in this investigation to compare the value of $d\gamma/dT$ for pure Ni and 304 stainless steel in the solid and liquid states since many investigators, in addition to ignoring the latent heat of fusion, assume $d\gamma/dT$ to be constant for a particular metal or alloy; and to be described by the Eötvös equation. There is no reason (*a priori*) for the Eötvös equation to be applicable in all cases of metals and alloys. While $d\gamma/dT$ has been shown to be nearly the same in the solid and liquid state for a few pure metals [5], there is no *a priori* reason for such an assumption in the case of metals and alloys in general. On the contrary, while a systematic (linear) response might be easily visualized for a crystalline solid, the transition to the liquid state would not allow for a continuation of any regular response related to an ordered lattice array. As a consequence, $d\gamma/dT$ is unlikely to be the same in both the solid and liquid states.

2. Experimental method

A commercial horizontal tube furnace was modified to be similar to the basic design features described by Humenik and Kingery [4]. A Pt–Rh thermocouple was positioned near the position of the sessile drop, and a 2 in. diameter, 0.25 in. thick optical window was fitted to one end of the furnace tube in order to photograph the equilibrium drop shape. As an initial check on the experimental procedure, drops of purified mercury and distilled water were placed on thoroughly degreased and washed glass slides carefully positioned in a level, horizontal plane in the hot zone of the furnace. A light source placed at the opposite end of the furnace tube allowed the drop profiles to be recorded in separate experiments using Tri-X film in a 35 mm camera employing a combination telephoto lens and close-up lens (1:2.8; $f = 135$ mm). From measurements of the sessile drop geometries shown in Fig. 2 and recorded at 25° C, the surface tension of water and mercury were calculated from Equation 1 and the tables of Koshavnik *et al.* [7] to be 74 and 478 erg cm^{-2} respectively. These values compared very favourably with accepted values of 72 erg cm^{-2} for water at 25° C [12] and

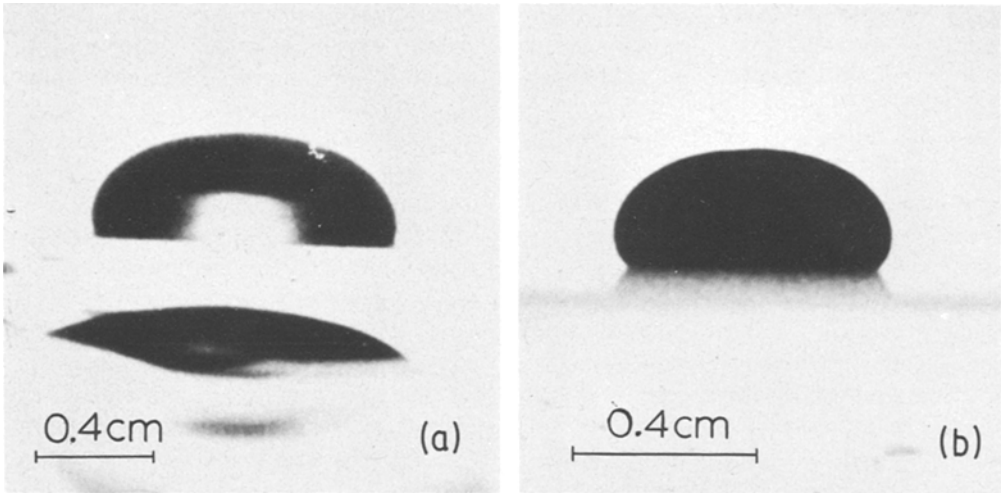

Figure 2 Sessile drops of water (a) and mercury (b) in the experimental system for calibration purposes.

476 erg cm^{-2} for mercury at 20° C [6, 13].

Small, weighed samples of nickel (99.97%) and 304 stainless steel (C = 0.07%, Mn = 1.90%, Si = 0.90%, Ni = 10.00%, Cr = 19.00%; balance Fe) were placed on metallurgically polished, high-purity thoria (ThO_2) and alumina (Al_2O_3) plaques respectively. These were placed on alumina support half-sections and pushed to the centre of the furnace in separate experiments, taking great care to keep the system completely level. At the outset of each experiment, the tube and sample were degassed by heating at 500° C while evacuating at ~0.1 μm. Following degassing, purified hydrogen gas (99.999%) was admitted into the furnace after passing through alkaline pyrogallol, sulphuric acid, and drierite chambers. The gas entered through the optical window end of the tube and was pressurized slightly using a mineral oil head in the opposite (exit) end of the furnace tube.

The furnace temperature was then raised and upon melting, the nickel on thoria or stainless steel on alumina assumed a sessile-drop shape as shown in Fig. 1. Photographs of the sessile drop were taken at the melting point and at temperatures above the melting point for each drop in separate experiments, allowing 0.5 h for equilibration at each temperature. This procedure was employed while raising the temperature over a narrow range above the melting point, and repeated upon decreasing the temperature back to the melting point. Photographs were taken at constant magnification and enlarged as in the calibration experiments demonstrated in Fig. 2.

3. Results

Because of the small size (<1 cm) of the liquid nickel sessile drops employed in this investigation, tabulated values of D and $d_m/2H$ (Equation 1 and Fig. 1) [7] were not available in the range measured for the sessile drop profiles. A plot of values of D versus $d_m/2H$ based upon the tables of Koshavnik *et al.* [7] was constructed and extended into the range of experimental values.

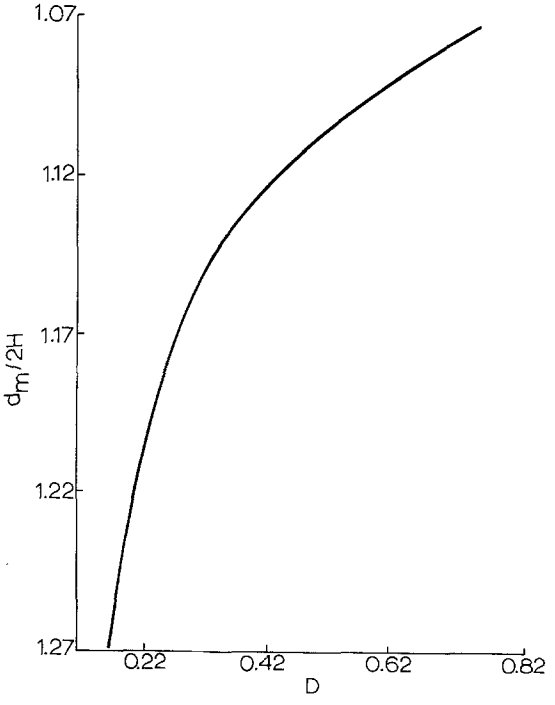

Figure 3 Variation of D (Equation 1) with respect to the ratio $d_m/2H$ (Fig. 1) from tabular data of Koshavnik *et al.* [7].

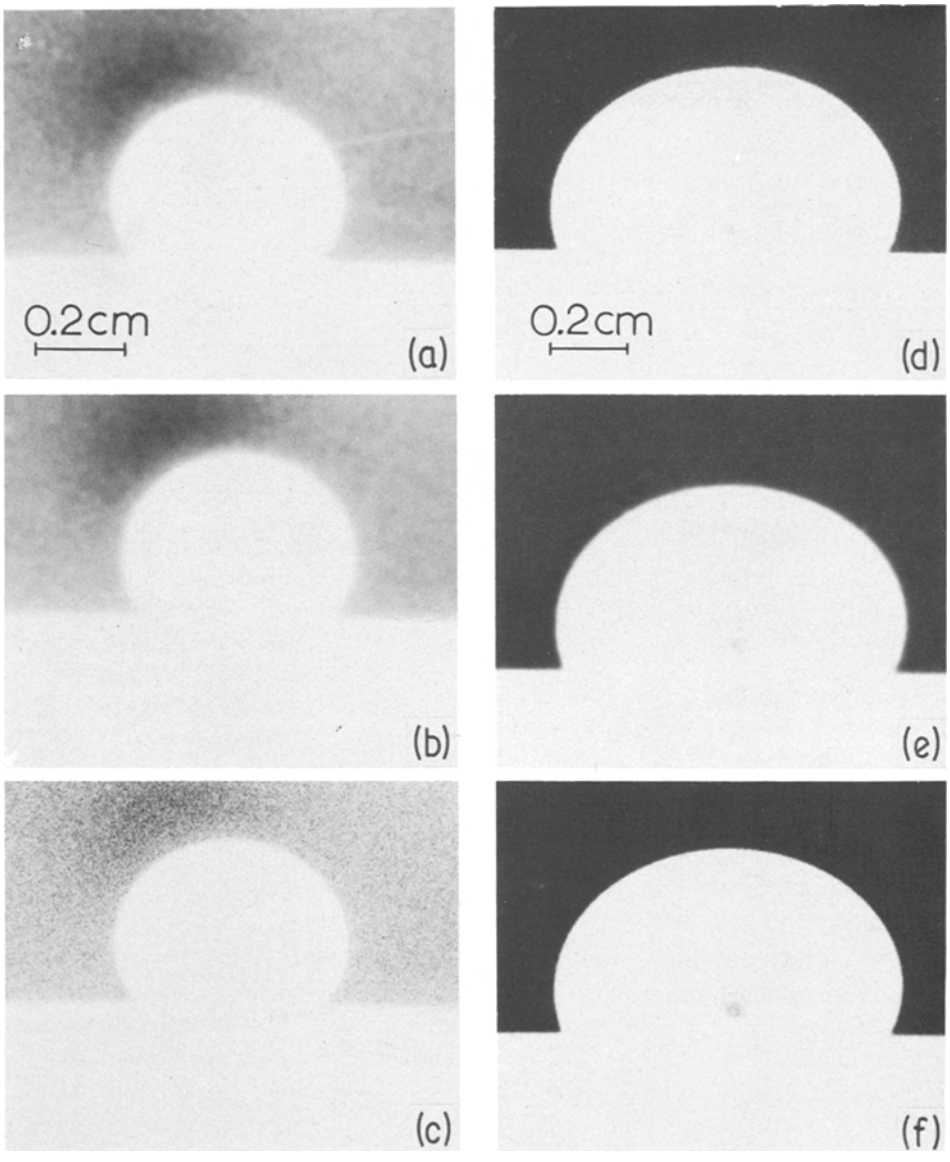

Figure 4 Sessile drops of nickel on a thoria substrate and 304 stainless steel on an alumina substrate at temperature, (a) nickel, 1455° C (m.p.); (b) nickel, 1480° C; (c) nickel, 15500° C; (d) stainless steel, 1475° C (m.p.); (e) stainless steel, 1485° C; (f) stainless steel, 1500° C.

This plot is reproduced in Fig. 3 which was applicable to both the nickel and stainless steel sessile drops recorded.

Fig. 4 illustrates the experimental photographs of nickel and stainless steel sessile drops from which the geometrical parameters d_m and H as well as the contact angle, Ω_c, were measured as a function of temperature. Tables I and II show the measured values of experimental parameters at temperature and the corresponding surface tension values calculated from Equation 1. Values of liquid nickel density in Equation 1 were taken to be $7.85\,g\,cm^{-2}$ from the previous work of Allen and Kingery [5]. This value was observed to decrease very slightly over the experimental temperature range and was assumed to be constant in calculations based on Equation 1. The density of the stainless steel was determined from the drop weight (at room temperature following the experiment) and the sessile drop volume, and found to change negligibly in the experimental temperature range from a value of $7.5\,g\,cm^{-3}$.

Fig. 5 provides some evidence of the extremely clean conditions which prevailed during the

TABLE I Experimental parameters for a nickel sessile drop on a solid thoria substrate

Temperature (° C)	d_m (cm)	$2H$ (cm)	$d_m/2H$	D	Ω_c (degrees)	γ_{LV} (erg cm^{-2})
1455 (m.p.)	0.562	0.521	1.078	0.730	135	1776
1460	0.561	1.520	1.079	0.725	133	1759
1470	0.560	0.519	1.080	0.715	132	1729
1480	0.559	0.518	1.081	0.705	130	1699
1490	0.558	0.516	1.082	0.700	129	1682
1500	0.557	0.515	1.084	0.690	127	1652

TABLE II Experimental parameters for a 304 stainless steel sessile drop on a solid substrate

Temperature (° C)	d_m (cm)	$2H$ (cm)	$d_m/2H$	D	Ω_c (degrees)	γ_{LV} (erg cm^{-2})
1475 (m.p.)	0.985	0.777	1.265	0.1700	119	1172
1480	0.974	0.768	1.271	0.1656	118	1115
1485	0.970	0.762	1.275	0.1628	117	1089
1490	0.968	0.751	1.288	0.1539	116	1025
1500	0.963	0.741	1.300	0.1466	114	966

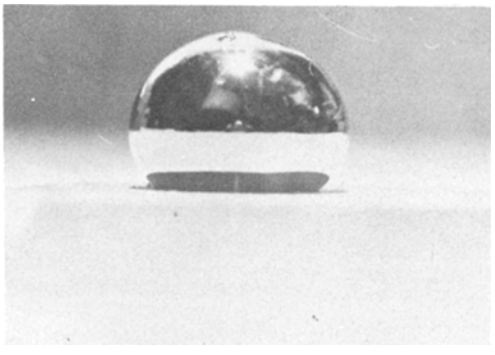

Figure 5 Photograph of nickel sessile drop in air at room temperature.

sessile drop experiments. No evidence of oxidation or other surface or interfacial reactions were observed for either the nickel on thoria or the stainless steel on alumina.

It can be observed from Tables I and II that both the nickel and stainless steel surface tensions decreased with increasing temperature above the melting point. Correspondingly, the contact angles in both the nickel–thoria and stainless steel–alumina systems decreased linearly with an increase in temperature above the melting point.

In Fig. 6 the experimental values of liquid nickel and stainless steel surface tensions (liquid surface free energies; Tables I and II) are plotted against the corresponding solid surface free energy curves determined from the previous work of Murr *et al.* [14] and Murr [1, 9] in the case of nickel, and Murr *et al.* [11] in the case of stainless steel. The discontinuity of surface free energy which occurs in each case at the melting point is representative of the associated latent heat of fusion,

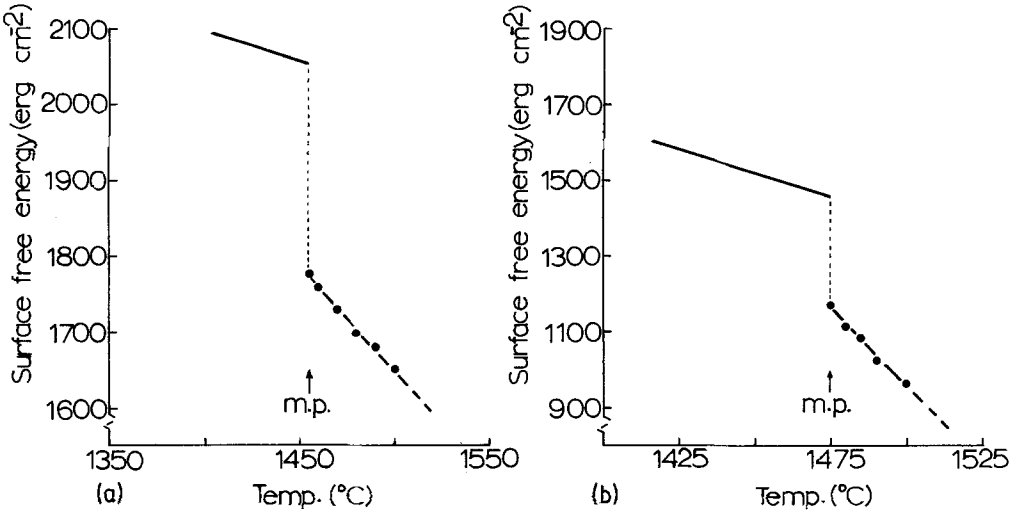

Figure 6 Temperature dependence of surface free energy and the solid–liquid surface transition energy in nickel and 304 stainless steel (a) nickel, (b) 304 stainless steel.

i.e. the energy per unit area of surface associated with the solid–liquid transition. It is noted from Fig. 6 that the latent heat of fusion for pure nickel is 292 erg cm^{-2} while in the case of 304 stainless steel it is found to be 284 erg cm^{-2}. The slope of the curves for both the nickel and stainless steel surface free energies are observed to be noticeably different in the liquid state as compared with the solid state. The value of dF_s/dT (where F_s is the solid surface free energy for pure nickel is -0.55 erg $cm^{-2}\,^{\circ}C^{-1}$ as compared with a value of $d\gamma_{LV}/dT = 1.76$ erg $cm^{-2}\,^{\circ}C^{-1}$ determined from Fig. 6. Similarly, the value of $dF_s/dT = -1.76$ erg $cm^{-2}\,^{\circ}C^{-1}$ for 304 stainless steel is considerably different from the value of $d\gamma_{LV}/dT = -2.48$ erg $cm^{-2}\,^{\circ}C^{-1}$ determined from Fig. 6.

4. Discussion

It is of interest to note that while the temperature coefficients of surface energy for nickel in the liquid and the solid states are different, they are both negative as expected on strictly thermodynamic grounds. Similarly, the negative temperature coefficient of surface free energy for solid stainless steel is the same in the liquid state. This is indicative not only of a clean surface at temperature but the absence of surface excess of any of the alloying or impurity components. It is also regarded as an indication of little preference for hydrogen adsorption at the free surface, or the formation of surface hydrides.

The present experiments for nickel, in addition to confirming the thermodynamic expectations for a pure metal, lend support to the previous proposals of surface contamination of nickel unrelated to hydrogen adsorption [15-17]. However, the present temperature coefficient of surface tension (-1.76 erg $cm^{-2}\,^{\circ}C^{-1}$) is nearly a factor of 2 greater than that previously measured by Allen and Kingery [5] for identical experimental conditions. Although the previous value of $d\gamma_{LV}/dT$ determined in the work of Allen and Kingery [5] was in closer agreement with the value of -0.85 erg $cm^{-2}\,^{\circ}C^{-1}$ computed from the Eötvös equation, there is no evidence, as stated earlier, the liquid metal surface tensions should be governed by the Eötvös condition. If the present value of $d\gamma_{LV}/dT$ is presumed to be correct, the surface tension variation with temperature would be expected to become nonlinear, or the value of $d\gamma_{LV}/dT$ would be expected to decrease at higher temperatures near the critical temperature since the surface tension at the critical temperature must be zero.

It is of interest that the value of $d\gamma_{LV}/dT$ for 304 stainless steel is greater than the value of dF_s/dT as in the case of pure nickel, and this may support the trend of the change in nickel. However, there is no corresponding experimental data for comparison in the case of stainless steel.

The values of the heats of fusion determined for both nickel and stainless steel from Fig. 6 are consistent with those measured previously by Allen and Kingery [5] for tin and copper, and shown to be characteristic of values which can be calculated for specific surface orientations [18].

Finally, it should be pointed out that consistent with Fig. 1, the adhesive energy for the liquid metal (or alloy)–solid ceramic systems studied can be determined from Tables I and II and the relation

$$E_{AD} = \gamma_{LV}(1 + \cos \Omega_c). \qquad (2)$$

Since γ_{LV} and Ω_c are tabulated as a function of temperature, E_{AD} can be determined as a function of temperature, and the value dE_{AD}/dT determined for the nickel–thoria system above the nickel melting point, or the stainless steel–alumina system above the stainless steel melting point.

5. Conclusions

(1) The temperature coefficients of surface tension for liquid nickel and 304 stainless steel have been determined to be -1.76 and -2.48 erg $cm^{-2}\,^{\circ}C^{-1}$ respectively in a narrow temperature range above the melting point.

(2) The liquid state temperature coefficients of surface free energy (surface tension) for pure nickel and stainless steel were observed to be linear but different from the corresponding temperature coefficients in the solid state.

(3) The latent heat of fusion determined by comparing the temperature coefficients of surface free energy in the solid and liquid states at the melting point were determined to be 292 and 284 erg cm^{-2} for pure nickel and type 304 stainless steel respectively.

(4) The contact angles for a liquid nickel sessile drop on thoria and a liquid stainless steel sessile drop on alumina were in each case observed to decrease with an increase in temperature above the melting point.

Acknowledgement

This work was supported in part by the Energy Research and Development Administration through a contract with Sandia Laboratories, Albuquerque, New Mexico.

References

1. L. E. MURR, "Interfacial Phenomena in Metals and Alloys" (Addison-Wesley, Reading, Mass., 1975).
2. F. BASHFORTH and S. C. ADAMS, "An Attempt to Test the Theories of Capillarity" (Cambridge University Press, Cambridge, 1883).
3. N. E. DORSEY, *J. Wash. Acad. Sci.* **18** (1928) 505.
4. M. HUMENIK and W. D. KINGERY, J. *Amer. Ceram. Soc.* 37 (1954) 18.
5. B. C. ALLEN and W. D. KINGERY, *Trans. Met. Soc. AIME* **215** (1959) 30.
6. W. BONFIELD, *J. Mater. Sci.* 7 (1972) 148.
7. A. Y. KOSHAVNIK, M. M. KUSANKUV and N.M. LUBMAN, *J. Phys. Chem. (Russian)* **27** (1953) 12 1887.
8. L. E. MURR, *Mater. Sci. Eng.* **12** (1973) 277.
9. *Idem. J. Mater. Sci.* **9** (1974) 1309.
10. M. E. FRASER, W–K LU, A. E. HAMILEC and R. MURARKA, *Met. Trans.* **2** (1971) 817.
11. L. E. MURR, G. I. WONG and R. J. HORYLEV, *Acta Met.* **21** (1973) 595.
12. J. J. BIKERMAN, "Physical Surfaces" (Academic Press, New York, 1970).
13. R. AVEYARD and D. A. HAYSON, "Introduction to the Principles of Surface Chemistry" (Cambridge University Press, Cambridge, 1973).
14. L' E. MURR, O. T. INAL and G. I. WONG, in "Electron Microscopy and Structure of Materials", edited by Thomas *et al.* (University of California Press, Berkely, 1972) p. 417.
15. U. M. AHMAD and L. E. MURR, *Scripta Met.* 8 (1974) 631.
16. W.–K. LU, *Scripta Met.* 8 (1974) 635.
17. R. MURARKA, W.–K. LU, and A. E. HAMIELEC, *Met. Trans.* **2** (1971) 2949.
18. A. BONDI, Chem. Rev. 52 (1953) 417.

Received 14 July and accepted 29 July 1975.